Xu *et al. Natural Products and Bioprospecting* (2026) 16:20
https://doi.org/10.1007/s13659-025-00575-y

Natural Products and Bioprospecting

ORIGINAL ARTICLE Open Access

Monoterpene indole alkaloids from the aerial parts of *Ophiorrhiza brevidentata* and their immunological activities

Fan Xu[1†], Zheng-Hui Li[1,2†], Meng-Lin Feng[1], Jia-Yu Jin[1], Bao-Bao Shi[1,2*] and Ji-Kai Liu[1,2*]

Abstract

Phytochemical study of the EtOAc extract of *Ophiorrhiza brevidentata* resulted in the discovery of 10 new monoterpene indole alkaloids (**1–10**), along with 13 known compounds (**11 — 23**). Compound **1** possess an unprecedented skeleton consisting of fused 6/5/6/7/6 polycyclic systems. The structural characterization of these compounds was achieved using Nuclear Magnetic Resonance, Mass Spectrometry and Quantum Chemical Calculations. Compounds **3–5** and **9** exhibited strong inhibition on lipopolysaccharide-induced B cell proliferation with IC_{50} values ranging from 3.6–9.1 μM with excellent selectivity indices (SI > 10).

Keywords Monoterpene indole alkaloids, ophiorrhiza brevidentata, immunological activity

Graphical abstract

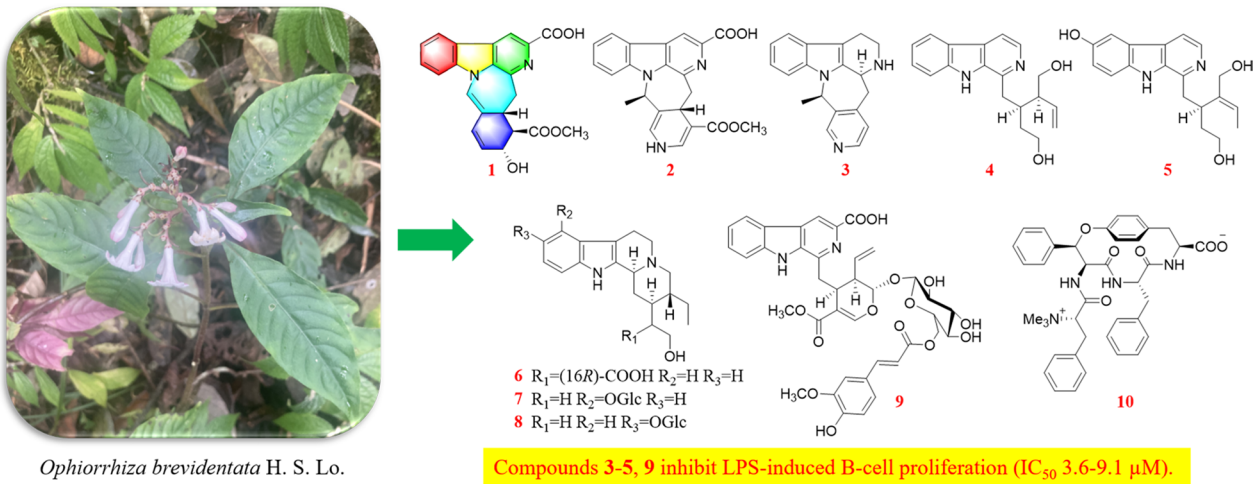

†Fan Xu and Zheng-Hui Li have authors contributed equally to this work.

*Correspondence:
Bao-Bao Shi
2021068@mail.scuec.edu.cn
Ji-Kai Liu
liujikai@mail.scuec.edu.cn
Full list of author information is available at the end of the article

Springer

1 Introduction

The immune system is a highly complex and finely regulated network of cells, tissues, and organs that plays a crucial role in maintaining the body's homeostasis and health. Its primary functions include identifying and eliminating foreign invaders as well as monitoring and removing abnormal or cancerous cells [1]. However, when the immune system fails to distinguish between foreign antigens and the body's own structures, it may produce autoantibodies that mistakenly attack healthy cells. This breakdown in self-tolerance can lead to the development of autoimmune diseases [2]. It is estimated that approximately 5–8% of the global population is affected by more than 150 different types of autoimmune disorders [3, 4]. Common autoimmune diseases encompass a spectrum of disorders, such as systemic lupus erythematosus, ankylosing spondylitis, Sjögren's syndrome, rheumatoid arthritis, and scleroderma, among others [5]. It is noteworthy that curative therapies are presently unavailable for numerous autoimmune disorders. Consequently, pharmacological intervention constitutes the mainstay of treatment [6]. However, most current immunosuppressive drugs cause severe side effects, including hepatotoxicity, nephrotoxicity, metabolic disorders, teratogenicity, and infertility [7–9]. Therefore, developing novel agents with higher efficacy and lower toxicity is urgently needed for treating autoimmune diseases.

Ophiorrhiza, a genus within the Rubiaceae family, comprises approximately 200 species, with 70 occurring in China [10]. Members of the Rubiaceae family are known to biosynthesize a wide array of secondary metabolites, such as indole alkaloids, anthraquinones, triterpenoids, and iridoids [11]. Among these, alkaloids represent the major biologically active compounds in *Ophiorrhiza* species, contributing to their diverse pharmacological properties such as anti-inflammatory, antioxidant, analgesic, anticancer, and antiviral effects [10]. Several novel, structurally distinct alkaloids exhibiting significant biological activities have been isolated from *O. japonica* in our preliminary research [12–15]. Notably, ophiorrhines A and B feature a unique bridged carbon framework formed via an intramolecular [4+2] Diels–Alder reaction [15]. Ophiorrhines F and G—key biogenetic precursors to ophiorrhines A and B—are characterized by an opened C-ring structure and have demonstrated pronounced and selective inhibition of B cell proliferation [12]. Consequently, a further investigation of other *Ophiorrhiza* species was undertaken in search of immunosuppressive alkaloids. This effort resulted in the isolation of ten previously undescribed alkaloids, named ophiorbrevines A–J (**1–10**), together with 13 known analogues (**11–23**) (Fig. 1), from title species. Herein, the isolation, structure elucidation, and immunosuppressive activities of these compounds are reported.

2 Results and discussion

Compound **1** was obtained as yellow powder, and its molecular formula was confirmed as $C_{22}H_{18}O_5N_2$ from ESIHRMS at *m/z* 391.12991 $[M+H]^+$ (calcd. for $C_{22}H_{19}N_2O_5^+$, 391.12885), with 13 degrees of unsaturation. The ^{1}H NMR spectrum (Table 1) exhibited characteristic signals corresponding to a 1,2-disubstituted phenyl ring, observed at δ_H 8.54 (1H, d, J=7.6 Hz), 7.58 (1H, t, J=7.6 Hz), 7.86 (1H, t, J=7.6 Hz), and 8.20 (1H, d, J=7.6 Hz). In addition, signals for four alkene protons were detected at δ_H 7.84 (1H, m), 5.92 (1H, dd, J=9.9, 2.1 Hz), 6.56 (1H, dd, J=9.9, 2.1 Hz), and 8.90 (1H, s), along with a methoxy signal at δ_H 3.93 (3H, s). Compound **1** showed 22 carbon signals in its ^{13}C NMR spectrum (Table 1), including one methoxy group, one methylene, eleven methines, and nine quaternary carbons. The HMBC correlation (Fig. 2) from H-9 to C-7/C-13, from H-12 to C-8, and H-6 to C-2/C-3/C-8 confirmed the presence of β-carboline moiety. The correlations from H-6 to the carboxyl carbon at δ_C 167.5 (C-22) suggested that a carboxyl group was located at C-5. The C_{14}–C_{19} fragment (C_{14}-C_{15}-C_{16}-C_{17}-C_{18}-C_{19}), which was established by ^{1}H–^{1}H COSY, HMBC, and HSQC spectra (Fig. 2), was determined to be connected to the β-carboline moiety at C-3. This connection was evidenced by key HMBC correlations from H-14 to C-2/C-3 and from H-15 to C-3. The key HMBC correlations from H-12/H-16 to C-20 and from H-19 to C-15 established the linkage between C-15 and C-20. Further HMBC correlations from H-15 to C-21 and from H-21 to C-2, C-13, C-15, and C-19, along with the chemical shift of C-21 (δ_C 122.2) and C-20 (δ_C 167.5), established the presence of a seven-membered nitrogen heterocycles with a double bond between C-20 and C-21. The HMBC correlations from both H-16 and H-24 to C-23 indicated that the ester group was attached to C-16. Based on biosynthetic pathway analysis, H-15 was assigned the β configuration. ROESY correlations between H-15 and H-17 (Fig. 4) further indicate that these protons were cofacial. The configuration of remaining H-16 was determined by comparing the experimental coupling constants of H-15/H-16 and H-16/H-17 with computed values. The calculated values for the 16*R** configuration [11.8 Hz ($^3J_{H\text{-}15/H\text{-}16}$) and 9.1 Hz ($^3J_{H\text{-}16/H\text{-}17}$), Fig. 3] showed closer agreement with the experimental data [11.0 Hz ($^3J_{H\text{-}15/H\text{-}16}$) and 9.2 Hz ($^3J_{H\text{-}16/H\text{-}17}$)] than those for the

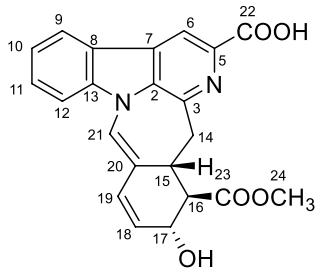

1*

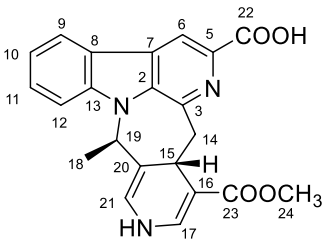

2*

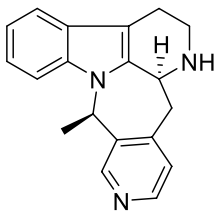

3*

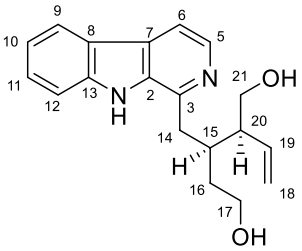

4*

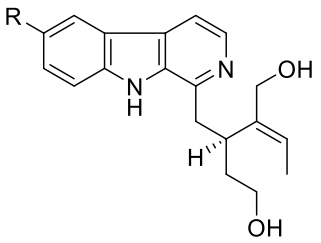

5* R = -OH
11 R = H

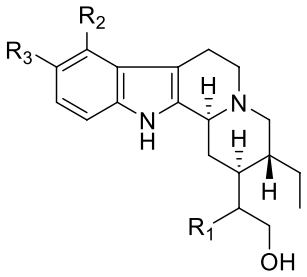

6* R_1 = α-COOH R_2 = H R_3 = H
7* R_1 = H R_2 = OGlc R_3 = H
8* R_1 = H R_2 = H R_3 = OGlc
12 R_1 = H R_2 = H R_3 = H

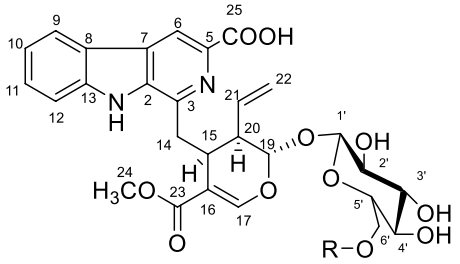

9* R =

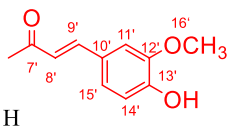

13 R = H

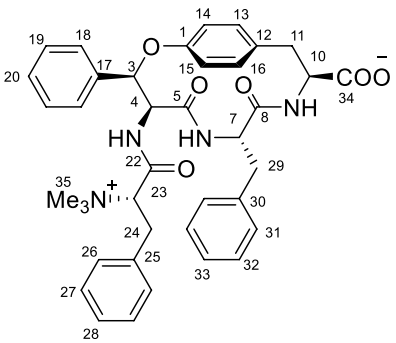

10*

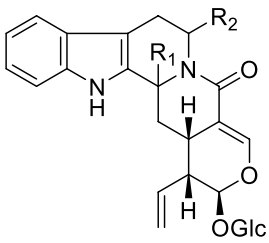

14 R_1 = α-H R_2 = β-COOH
15 R_1 = α-H R_2 = H
16 R_1 = β-H R_2 = H

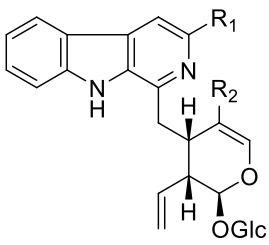

17 R_1 = COOH R_2 = $COOCH_3$
18 R_1 = H R_2 = $COOCH_3$
19 R_1 = H R_2 = COOH

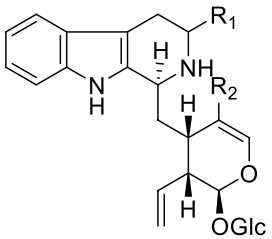

20 R_1 = H R_2 = COOH
21 R_1 = β-COOH R_2 = $COOCH_3$

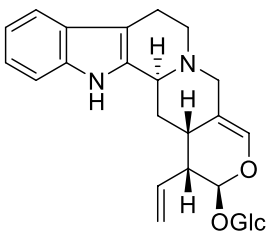

22

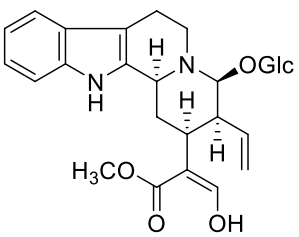

23

Fig. 1 Chemical structures of compounds **1–23**

Table 1 ^{1}H and ^{13}C NMR spectroscopic data of compounds **1–3** (DMSO and CD_3OD)

No	1[a]		2[a]		3[b]	
	δ_C, type	δ_H, mult (*J* in Hz)	δ_C, type	δ_H, mult (*J* in Hz)	δ_C, type	δ_H, mult (*J* in Hz)
2	133.6, C		135.3, C		135.7, C	
3	143.9, C		143.8, C		48.3, CH	4.39, d (6.8)
5	137.1, C		136.9, C		49.8, CH_2	3.16, ddd (11.4, 5.1, 2.7)
						3.06, td (10.7, 4.3)
6	115.1, CH	8.90, s	114.9, CH	8.76, s	22.5, CH_2	2.93, tdd (10.3, 5.2, 2.1)
						2.88, m
7	129.8, C		129.7, C		108.3, C	
8	121.4, C		121.8, C		128.2, C	
9	122.2, CH	8.54, d (7.6)	122.0, CH	8.39, d (7.5)	118.8, CH	7.41, d (8.0)
10	122.2, CH	7.58, t (7.6)	120.6, CH	7.35, t (7.5)	119.9, CH	6.98, t (8.0)
11	129.1, CH	7.86, t (7.6)	128.7, CH	7.67, t (7.5)	122.2, CH	7.06, t (8.0)
12	111.2, CH	8.20, d (7.6)	111.9, CH	7.85, d (7.5)	111.9, CH	7.30, d (8.0)
13	140.1, C		140.8, C		138.4, C	
14	41.6, CH_2	3.61, dd (15.3, 10.6)	48.1, CH_2	3.04, m	34.9, CH_2	3.44, dd (17.4, 4.3)
		3.44, d (15.3)		3.41, dd (16.0, 2.8)		2.83, m
15	36.5, CH	3.35 dd (11.0, 10.6)	28.5, CH	4.02, dd (11.7, 2.9)	144.8, C	
16	55.3, CH	2.79, dd (11.0, 9.2)	99.3, C		125.4, CH	7.24, d (5.2)
17	67.73, CH	4.58, d (9.2)	138.0, CH	7.42, d (5.5)	147.3, CH	8.27, d (5.2)
18	130.6, CH	5.92, dd (9.9, 2.1)	18.1, CH_3	1.35, d (6.6)	16.7, CH_3	1.45, d (7.0)
19	128.3, CH	6.56, dd (9.9, 2.1)	55.9, CH	5.78, q (6.5)	57.4, CH	4.41, q (7.0)
20	122.4, C		114.1, C		138.4, C	
21	122.2, CH	7.84, s	124.2, CH	6.70, d (4.3)	149.0, CH	8.37, s
22	167.5, C		167.1, C			
23	174.5, C		167.6, C			
24	52.0, CH_3	3.93, s	50.9, CH_3	3.68, s		
N–H				8.80, s		

[a] Measured on 600/150 MHz in DMSO-d6. [b]Measured on 500/125 MHz in CD_3OD

16*S** configuration [5.7 Hz ($^{3}J_{H\text{-}15/H\text{-}16}$) and 2.7 Hz ($^{3}J_{H\text{-}16/H\text{-}17}$)]. Finally, the absolute configuration of compound **1** was assigned as 15*R*,16*R*,17*R* by comparing the calculated and experimental electronic circular dichroism (ECD) spectra (Fig. 5).

The molecular formula of compound **2**, an orange powder, was established as $C_{22}H_{19}O_4N_3$ from ESIHRMS data, which showed an $[M+H]^+$ ion at *m/z* 390.14465 (calcd 390.14483). This formula corresponds to 15 degrees of unsaturation. The UV spectrum exhibited absorption maxima at 210, 240, and 270 nm, which were distinct from those of compound **1**. Its ^{1}H NMR spectrum showed the presence of one methyl group (δ_H 1.35), one methoxy group (δ_H 3.68), and seven alkene protons (δ_H 8.76, 8.39, 7.35, 7.67, 7.85, 7.42, and 6.70) (Table 1). Its ^{13}C NMR spectrum exhibited 22 distinct resonances, accounting for two methyl groups, one methylene, nine methines, and ten quaternary carbons (including two carbonyls). Careful analysis of the NMR data (Table 1) revealed that **2** was very similar to Mappianine B [16]. The key structural difference between the two compounds is the lack of an ethyl group at N-25 and the addition of a carboxyl group at C-5 in compound **2**. This assignment was supported by HMBC correlations from H-N_{25} to C-16 (δ_C 99.3)/C-20 (δ_C 114.1) and from H-6 to C-22 (δ_C 167.1) in spectrum. The combined analysis of the ROESY spectrum (Fig. 4), which showed correlations from H-18 to H-15, and the calculated ECD spectra (Fig. 5) confirmed the absolute configuration of **2** as 15*S*,19*R*.

Compound **3** was obtained as yellow powder, and its molecular formula was determined to be $C_{19}H_{19}N_3$ from ESIHRMS, exhibiting a protonated ion peak at *m/z* 290.16501 $[M+H]^+$ (calcd for $C_{19}H_{20}N_3^+$, 290.16517), consistent with 12 degrees of unsaturation. The ^{1}H NMR spectrum exhibited signals characteristic of an indole moiety, including resonances at δ_H 7.41 (1H, d, J=8.0 Hz), 6.98 (1H, t, J=8.0 Hz), 7.06 (1H, t, J=8.0 Hz), and 7.30 (1H, d, J=8.0 Hz), along with a methyl signal observed at δ_H 1.45 (3H, d, J=7.0 Hz). Compound **3**

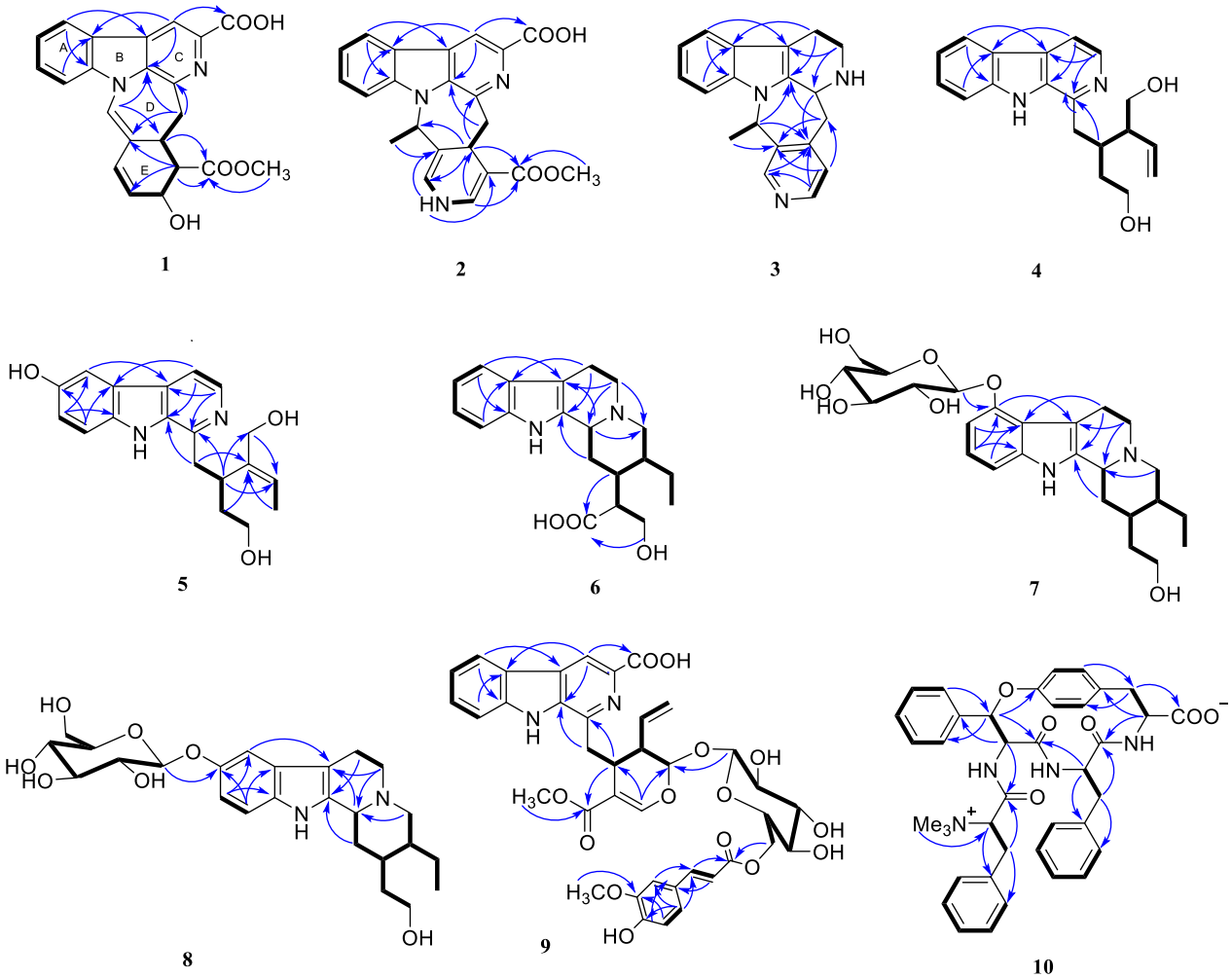

Fig. 2 Key ^{1}H-^{1}H COSY and HMBC correlations for **1**–**10**

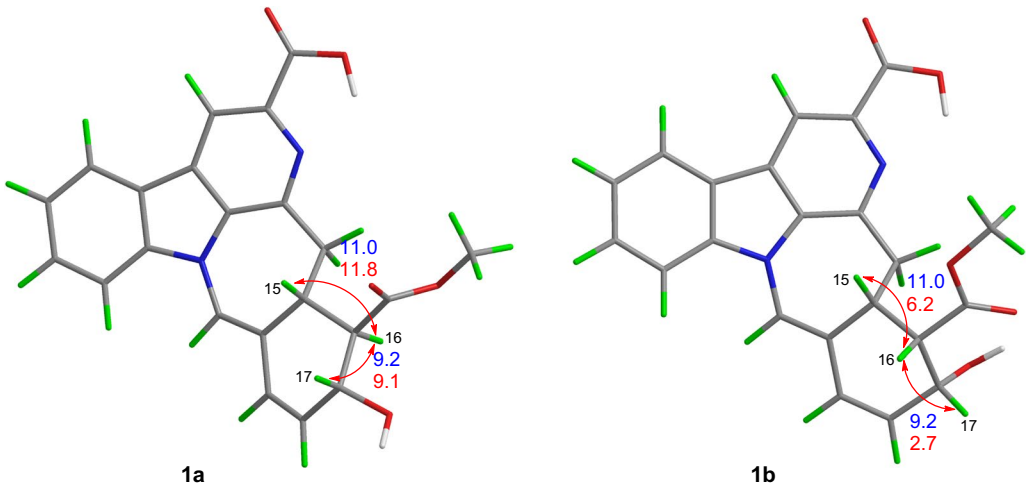

Fig. 3 Calculated (red) and experimental (blue) spin–spin coupling constants of **1a** and **1b**

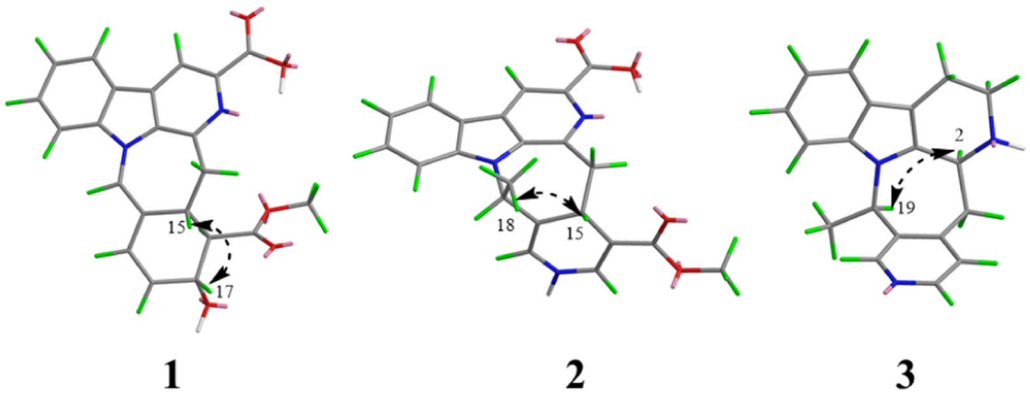

Fig. 4 Key ROESY correlations for **1–3**

was characterized as a yellow powder with the molecular formula $C_{19}H_{19}N_3$ (12 degrees of unsaturation), as evidenced by ESIHRMS (*m/z* 290.16501 $[M+H]^+$; calcd 290.16517). The ^{1}H NMR data supported the presence of an indole ring system [δ_H 7.41 (1H, d, J=8.0 Hz), 6.98 (1H, t, J=8.0 Hz), 7.06 (1H, t, J=8.0 Hz), 7.30 (1H, d, J=8.0 Hz)], along with a methyl doublet at δ_H 1.45 (3H, d, J=7.0 Hz). Analysis of the ^{13}C NMR and DEPT spectra indicated the presence of six quaternary carbons (δ_C 135.7, 108.3, 128.2, 138.4, 144.8, 138.4), nine methines (δ_C 48.3, 118.8, 119.9, 122.2, 111.9, 125.4, 147.3, 57.4, 149.0), three methylenes (δ_C 49.8, 22.5, 34.9), and one methyl group (δ_C 16.7). The NMR data for compound **3** closely matched those of 3,14-dihydrodecussine [17], with the key difference being the absence of an N_4-methyl resonance. This observation is consistent with the ESIHRMS data, which indicated a molecular weight 14 units lower for compound **3**, supporting the lack of the N-methyl group. The ROESY correlation observed between H-19 and H-3confirmed that these protons are co-facial (Fig. 4). This observation, combined with the biosynthesis pathway, allows the absolute configuration to be inferred to be 3*S*,19*R*.

Compound **4** was characterized as a yellow powder with the molecular formula $C_{19}H_{22}N_2O_2$ (10 degrees of unsaturation), as determined from ESI-HRMS (*m/z* 311.17517 $[M+H]^+$; calcd 311.17540). The ^{1}H NMR data were consistent with the presence of a β-carboline moiety, evident from a characteristic set of six aromatic proton signals [δ_H 8.22 (1H, d, J=5.4 Hz, H-5), 7.95 (1H, d, J=5.4 Hz, H-6), 8.16 (1H, d, J=8.0, H-9), 7.25 (1H, ddd, J=8.0, 6.9, 1.1 Hz, H-10), 7.55 (1H, ddd, J=8.0, 6.9, 1.1 Hz, H-11), 7.58 (1H, d, J=8.0,, H-12)]. Additionally, signals for a terminal double bond were observed at δ_H 5.20 (1H, dd, J=10.4 2.0 Hz, H-18a), 5.10 (1H, ddd, J=17.2, 2.0, 0.9 Hz, H-18b), 5.85 (1H, ddd, J=17.2, 10.4, 8.9 Hz, H-19). Analysis of the ^{13}C NMR and DEPT data identified 19 carbon resonances, comprising five

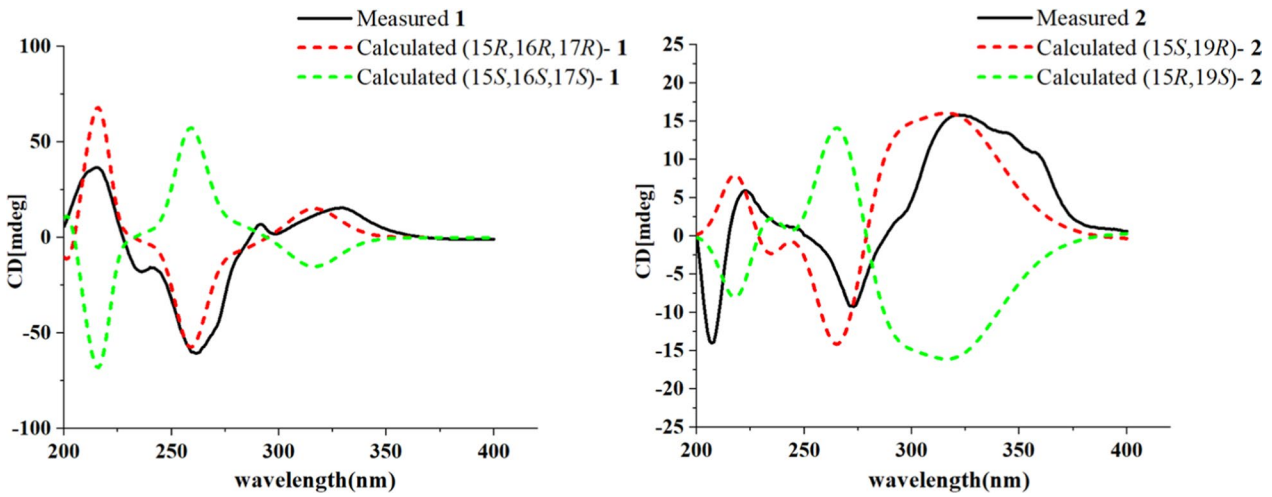

Fig. 5 ECD calculations of **1** and **2**

methylenes, nine methines, and five quaternary carbons (Table 2). The ^{1}H and ^{13}C NMR data of **4** were structurally similar to those of the known compound 10-hydroxy-iso-deppeaninol [18], except for the absence of hydroxyl substitution at C-10 in compound **4**. This presumption was confirmed by the ^{1}H-^{1}H COSY correlations of H-9/H-10/H-11/H-12. Considering the biogenetic relationship between **4** and 10-hydroxy-iso-deppeaninol, their stereochemical structures were predicted to be identical. Consequently, the absolute configuration of **4** was assigned as 15*R*,20*S*.

Compound **5** was characterized as a yellow powder with the molecular formula $C_{19}H_{22}N_2O_3$ (10 degrees of unsaturation), as determined by ESI-HRMS (*m/z* 327.17010 $[M+H]^+$; calcd 327.17032). The ^{1}H NMR spectrum supported the *β*-carboline structure, showing key proton signals at δ_H 8.09 (1H, d, *J*=5.4 Hz, H-5), 7.80 (1H, d, *J*=5.4 Hz, H-6), 7.46 (1H, m, H-9), 7.09 (1H, dd, *J*=8.8, 2.4 Hz, H-11), and 7.39 (1H, d, *J*=8.8 Hz, H-12). Furthermore, the signal for H-19 at δ_H 5.37 (1H, dd, *J*=6.8 Hz) confirmed the presence of a double bond. The ^{13}C NMR and DEPT spectra (Table 2) showed one methyl group, four methylene groups, seven methine groups, and seven quaternary carbons. The ^{1}H and ^{13}C NMR spectra of **5** showed a close resemblance to those of **12**, suggesting that they share the same core structure. The only difference was the additional hydroxyl substitution at C-10 in **5**, which was unambiguously confirmed by the observed HMBC correlations from H-12, H-11, and H-9 to the oxygenated carbon at C-10.

Compound **6** was characterized as a yellow powder with the molecular formula $C_{20}H_{26}N_2O_3$ (9 degrees of unsaturation), as assigned from the ESIHRMS signal at *m/z* 343.20145 $[M+H]^+$ (calcd 343.20162). The structural features were supported by NMR data (Table 3): the ^{1}H NMR spectrum indicated an indole moiety and a methyl group, while the ^{13}C NMR and DEPT spectra detailed the carbon skeleton, consisting of five quaternary carbons, eight methines, six methylenes, and one methyl group. Comparing their NMR data, compound **6** had very similar structure to that of known compound, dihydro-18,19 sitsirikine [19], and the only difference in their structures was the existence of a carboxyl group in compound **6** instead of a ester group in dihydro-18,19 sitsirikine. This conclusion was confirmed by the key HMBC correlation from H-15/H-17 to C-22 (δ_C 179.5) (Fig. 2).

The molecular formula of compound **7**, a yellow amorphous powder, was established as $C_{25}H_{36}N_2O_7$ (9 degrees of unsaturation) from high-resolution mass data. The ESIHRMS spectrum showed an $[M+H]^+$ ion at *m/z* 477.25934, in excellent agreement with the calculated value of 477.25953 for $C_{25}H_{37}N_2O_7^+$. The ^{1}H NMR spectrum (Table 3) displayed characteristic signals

Table 2 ^{1}H and ^{13}C NMR spectroscopic data of compounds **4–5** (CD_3OD)

No	4[a]		5[b]	
	δ_C, type	δ_H, mult (*J* in Hz)	δ_C, type	δ_H, mult (*J* in Hz)
2	136.5, C		137.3, C	
3	146.3, C		145.8, C	
5	138, CH	8.22, d (5.4)	136.7, CH	8.09, d (5.4)
6	114.2, CH	7.95, d (5.4)	114.2, CH	7.80, d (5.4)
7	130.2, C		130.0, C	
8	122.7, C		123.2, C	
9	122.6, CH	8.16, d (8.0)	106.7, CH	7.46, d (2.4)
10	120.8, CH	7.25, t (8.0)	152.3, C	
11	129.5, CH	7.55, t (8.0)	119.6, CH	7.09, dd (8.8, 2.4)
12	112.9, CH	7.58, d (8.0)	113.5, CH	7.39, d (8.8)
13	142.6, C		137.1, C	
14	37.5, CH_2	3.18, m	39.3, CH_2	3.33, m
15	36.4, CH	2.54, tt (7.6, 3.8)	36.7, CH	3.38, m
16	34.1, CH_2	1.81,m	36.9, CH_2	1.96, m
		1.51, m		1.87, m
17	61.5, CH_2	3.46, m	61.2, CH_2	3.60, m
				3.50, m
18	118.6, CH_2	5.20, dd, (10.4, 2.0)	12.8, CH_3	1.00, d (6.9)
		5.10, ddd (17.2, 2.0, 0.9)		
19	138.3, CH	5.85, ddd (17.2, 10.4, 8.9)	126.6, CH	5.37, q (6.9)
20	50.9, CH	2.29, m	140.0, C	
21	64.5, CH_2	3.62, d (6.8)	65.5, CH_2	4.26, m
				4.04, d (12.3)

[a] Measured on 600/150 MHz. [b]Measured on 500/125 MHz

consistent with a monosubstituted indole system, including resonances at δ_H 6.67 (1H, d, *J*=7.8 Hz), 6.90 (1H, t, *J*=7.8 Hz), and 6.94 (1H, t, *J*=7.8 Hz), along with a methyl signal at δ_H 0.94 (3H, d, *J*=7.5 Hz). The ^{13}C NMR and DEPT spectra revealed the presence of five quaternary carbons, eleven methines, eight methylenes, and one methyl group. Careful analysis of the NMR data revealed that the structure of compound **7** was highly similar to that of **6**, with the key structural differences being the absence of the carboxyl group and the appearance of a glycosyl substitution at C-9 in compound **7**. This presumption was confirmed by the ^{1}H-^{1}H COSY correlations of H-3/H-14/H-15/H-16/H-17 and the key HMBC correlation from the anomeric proton H-1' to C-9 (δ_C 153.1). The *J* values (*J*=7.4 Hz) of the anomeric proton revealed a *β*-configuration of the glucose residue. Furthermore, the stereocenters at C-3, C-15 and C-20 in **7** were assigned as identical to those in **6**, consistent with a biosynthetic pathway that does not involve bond cleavage at these positions.

The molecular formula of compound **8**, a yellow amorphous powder, was determined to be $C_{25}H_{36}N_2O_7$,

Table 3 ^{1}H and ^{13}C NMR Spectroscopic Data of Compounds **6 – 8** (CD_3OD)

No	6[a]		7[a]		8[b]	
	δ_C, type	δ_H, mult (*J* in Hz)	δ_C, type	δ_H, mult (*J* in Hz)	δ_C, type	δ_H, mult (*J* in Hz)
2	132, C		134.6, C		137.1, C	
3	62.3, CH	3.99, t (9.5)	61.7, CH	3.22 m	61.7, CH	3.21, d (11.6)
5	53.8, CH_2	3.53, m	54.7, CH_2	3.04 m	54.4, CH_2	3.09, t (5.8)
		3.12, m		2.57 td (11.7, 4.6)		2.57 td (11.5, 4.6)
6	20.8, CH_2	3.11, m	24.4, CH_2	3.23 m	22.3, CH_2	2.93, m
		2.88, d (11.5)		3,03 m		2.67, dd (15.3, 4.4)
7	107.1, C		107.7, C		107.9, C	
8	127.7, C		119.5, C		128.7, C	
9	118.9, CH	7.39, d (7.6)	153.1, C		106.5, CH	7.15, d (2.4)
10	120.3, CH	6.99, t (7.6)	104.4, CH	6.67, d (7.8)	153.0, C	
11	122.9, CH	7.07, t (7.6)	122.5, CH	6.90, t (7.8)	113.7, CH	6.90, dd (8.7, 2.4)
12	112.3, CH	7.27, d (7.6)	106.8, CH	6.94, d (7.8)	112.2, CH	7.16, d (8.7)
13	138.4, C		139.7, C		134.5, C	
14	30.4, CH_2	2.49, d (9.5)	35.7, CH_2	2.43, d (13.0)	35.7, CH_2	2.42, dt (13.2, 3.1)
		1.88, d (10.0)		1.19, m		1.21, m
15	39.4, CH	1.88, d (10.0)	38.1, CH	1.44, m	38.1, CH	1.4, m
16	51.2, CH	2.83, t (7.8)	36.6, CH_2	1.98, m	36.6, CH_2	1.96, dtd, (13.6, 7.8, 2.4)
				1.30, m		1.31, m
17	62.8, CH_2	3.89, dd (10.9, 6.8)	60.6, CH_2	3.72, ddd (12.7, 7.9, 4.8)	60.6, CH_2	3.67, m
		3.67, dd (11.0, 7.8)		3.66, m		
18	10.3, CH_3	0.94, t (7.5)	11.3, CH_3	0.94, t (7.5)	11.3, CH_3	0.93, t (7.6)
19	23.7, CH_2	1.88, d (10.0)	24.5, CH_2	1.71, m	24.5, CH_2	1.70, dqd (15.2, 7.5, 2.3)
		1.39, dt (14.7, 7.7)		1.17, m		1.16, m
20	39.2, CH	2.02, m	42.8, CH	1.45, m	42.9, CH	1.43, m
21	59.6, CH_2	3.46, d (11.5)	61.4, CH_2	3.05, m	61.4, CH_2	3.07, dd (11.6, 3.1)
		2.66, s		2.13, t (11.0)		2.13, t (10.1)
22	179.5, C					
1′			102.2, CH	5.05, d (7.4)	104.4, CH	4.81, m
2′			75.3, CH	3.48, dd (9.2, 7.4)	75.2, CH	3.43, m
3′			78.5, CH	3.45, t (8.6)	78.1, CH	3.43, m
4′			71.4, CH	3.37, m	71.5, CH	3.37, m
5′			78.1, CH	3.40, m	78.1, CH	3.37, m
6′			62.6, CH_2	3.86, dd (12.1, 2.2)	62.6, CH_2	3.87, d (11.9)
				3.68, d (5.3)		3.69, m

[a] Measured on 600/150 MHz. [b]Measured on 600/125 MHz

corresponding to 9 degrees of unsaturation. This assignment was supported by ESIHRMS, which displayed an $[M+H]^+$ ion at *m/z* 477.26126 (calcd 477.25953 for $C_{25}H_{36}N_2O_7^+$). The ^{1}H and ^{13}C NMR data (Table 3) of **8** closely resembled those of **7**, indicating an identical core structure. The key difference was the position of the glycosyl substitution, which was located at C-10 in **8** instead of C-9 as in **7**. This hypothesis was supported by the ^{1}H-^{1}H COSY correlations of H-11/H-12 and the key HMBC correlation from the anomeric proton H-1' to C-10 (δ_C 153.0).

The molecular formula of compound **9**, a yellow amorphous powder, was determined to be $C_{38}H_{38}N_2O_{14}$, consistent with 21 degrees of unsaturation. This assignment was supported by ESIHRMS, which displayed an $[M+H]^+$ ion at *m/z* 747.24042 (calcd 747.23958 for $C_{38}H_{38}N_2O_{14}^+$). The ^{1}H NMR spectra of **9** showed two methoxy protons at δ_H 2.85 (3H, s, H-24) and 3.43 (3H, s H-16'). The ^{13}C NMR and DEPT spectra (Table 4) of **9** showed two methoxy groups (δ_C 55.8, 51.4), three methylenes, twenty methines, and thirteen quaternary carbons. Careful analysis of the NMR data revealed that **9**

was very similar to 6'-trans-feruloyl-6'-lyaloside [20]. The key structural difference between the two compounds is the addition of a carboxyl group at C-5 in compound **10**. This assignment was supported by HMBC correlations from H-6 to C-24 (δ_C 166.7) in spectrum. Given the close biogenetic relationship and shared biosynthetic origin between compound **9** and 6'-trans-feruloyl-6'-lyaloside, their stereochemical structures were inferred to be identical. Consequently, the absolute configuration of **9** was thus assigned as 15*S*,19*S*,20*R*.

Compound **10** was obtained as yellow amorphous powder, and its molecular formula was confirmed as $C_{39}H_{42}N_4O_6$ from ESIHRMS at *m/z* 663.31771 $[M+H]^+$ (calcd. for $C_{39}H_{43}N_4O_6^+$, 663.31885), with 21 degrees of unsaturation. The ^{1}H NMR data (Table 5) showed signals for nineteen aromatic protons, three N-methyl groups, and four amino methines. The ^{13}C NMR spectrum revealed signals consistent with twenty-four aromatic carbons, four carbonyl groups, five methines, three methylenes, and three methyl groups. Through detailed analysis of the spectroscopic data, the structure of 11 was elucidated and found to be highly similar to that of ophiorrhisine A [21], a compound isolated from *Ophiorrhiza* nutans. The key structural difference was the lack of a hydroxyl substitution at the C-28 in compound **10**.

In addition to the new compounds mentioned above, 13 known compounds were obtained and identified as deppeaninol (**11**) [22], (–)-dihydrocorynanthenol (**12**) [23], desoxycordifoline (**13**) [24], 3*α*-5*α*-tetrahydrodeoxycordifoline lactam (**14**) [25], strictosamide (**15**) [26], vincosamide (**16**) [27], desoxycordifoline (**17**) [28], lyaloside (**18**) [29], lyalosidie acid (**19**) [30], strictosidinic acid (**20**) [31], 5*α*-carboxystrictosidine (**21**) [32], deoxystrictosamide (**22**) [33], and turbinatine (**23**) [34], by comparison with literature data.

The immunoactivity of the compounds **1** and **3–10** was determined by ^{3}H-TdR incorporation method. The level of lymphocyte response to the stimulus could be inferred based on the amount of isotope incorporated into the cell (as measured by liquid scintillation) and compared with the active control drug immunosuppressant cyclosporin A (CsA), and the results were shown in Table 6. Based on a comprehensive analysis of cytotoxicity (MTT assay) and immunomodulatory activity, compounds **3–5** and **9** strongly inhibited lipopolysaccharide-induced B cell proliferation, with IC_{50} values ranging from 3.6 to 9.1 μM, and demonstrated excellent selectivity (SI > 10). Meanwhile, compounds **1**, **3–5**, and **10** exhibited moderate inhibitory activity against concanavalin A-induced T cell proliferation, with IC_{50} values from 15.7 to 58.6 μM.

Table 4 ^{1}H and ^{13}C NMR Spectroscopic Data of Compound **9** (CD_3OD)

No	9		No	9	
	δ_C, type	δ_H, mult (*J* in Hz)		δ_C, type	δ_H, mult (*J* in Hz)
2	136.6, C		23	168.3, C	
3	150.0, C		25	166.7, C	
5	137.9, C		24	51.4, CH_3	2.85, s
6	146.3, CH	8.70, s	1′	101.7, CH	4.75, d (7.8)
7	133.1, C		2′	74.4, CH	3.29, m
8	122.4, C		3′	77.9, CH	3.45, m
9	123.8, CH	8.29, d (7.9)	4′	72.5, CH	3.35, m
10	122.5, CH	7.40, t (7.9)	5′	76.0, CH	3.64, td (9.1, 2.6)
11	131.8, CH	7.72, t (7.9)	6′	64.2, CH_2	4.85, d (9.8)
12	113.4, CH	7.67, d (7.9)			4.33, dd (11.9, 2.5)
13	144.5, C		7′	168.9, C	
14	34.8, CH_2	3.45, t (9.1)	8′	115.0, CH	6.39, d (15.9)
15	37.1, CH	3.36, t (5.7)	9′	147.3, CH	7.55 d (15.9)
16	109.2, C		10′	126.6, C	
17	155.4, CH	7.46, s	11′	110.3, CH	6.69, d (2.2)
18			12′	148.6, C	
19	97.9, CH	5.75, d (9.2)	13′	150.0, C	
20	45.5, CH	2.64, td (8.7, 4.9)	14′	115.5, CH	5.92, dd (8.2, 2.0)
21	135.1, CH	5.92, m	15′	123.6, CH	6.64, dd (8.2, 2.0)
22	120.0, CH_2	5.30, dd (13.8,7.7)	16′	55.8, CH_3	3.43, s

Measured on 600/150 MHz

Table 5 ^{1}H and ^{13}C NMR Spectroscopic Data of Compound **10** (CD_3OD)

No	10		No	10	
	δ_C, type	δ_H, mult (*J* in Hz)		δ_C, type	δ_H, mult (*J* in Hz)
1	156.6, C		20	130, CH	7.33, m
3	81.4, CH	5.78, d (9.1)	22	165.6, C	
4	58.3, CH	4.99, d (9.1)	23	75.3, CH	4.41, d (8.4)
5	169.8, C		24	34.6, CH_2	3.11, dd (14.7, 6.2)
7	54.4, CH	4.64, dt (7.4, 3.9)			2.87, dd (14.7, 7.9)
8	170, C		25	135.9, C	
10	57.4, CH	4.77, dd (11.2, 6.7)	26	130.3, CH_2	7.17, m
11	40.8, CH_2	3.51, dd (13.4, 6.7)	27	130.1, CH_2	7.18, m
		2.71, dd (13.4, 11.1)	28	128.6, CH	7.07, tt (6.6, 2.0)
12	133.3, C		29	40.3, CH_2	2.58, dd (14.4, 6.7)
13	131.9, CH	7.15, m			2.43, dd (14.4, 6.7)
14	114.8, CH	7.13, m	30	137.6, C	
15	120.4, CH	6.84, m	31	130.2, CH_2	6.85, m
16	133.7, CH	6.85, m	32	129.2, CH	6.91, t (7.6)
17	139.7, C		33	127.4, CH	6.72, t (7.3)
18	130.4, CH_2	7.61, d (7.0)	34	178.1, C	
19	129.6, CH_2	7.37, dd (8.1, 6.7)	35	52.8, CH_3	2.64, s

Measured on 600/150 MHz

3 Experimental section

General Experimental Procedures NMR spectroscopic data were acquired using Bruker Avance III 600 MHz and 500 MHz spectrometers. UV measurements were conducted on a UH-5300 UV–vis spectrophotometer. CD profiles were obtained with a Chirascan-plus circular dichroism spectrometer. Column chromatography (CC) was carried out with silica gel (Qingdao Marine Chemical Ltd., China), RP-18 gel (Fuji Silysia Chemical Ltd., Japan), and Sephadex LH-20 (Pharmacia Fine Chemical Co., Ltd., Sweden). TLC analysis was performed on GF 254 plates (Qingdao Haiyang Chemical Co., Ltd., China), and spots were visualized using Dragendorff's reagent. Medium-pressure liquid chromatography (MPLC) separations were executed on a Biotage SP1 system. HPLC purification was conducted using an Agilent 1260 series system equipped with analytical semi-preparative or preparative Sunfire C_{18} columns (dimensions: 4.6×150 mm and 19×250 mm, respectively).

Plant Material Ophiorrhiza brevidentata H. S. Lo was collected from Baoshan and Tengchong County, Yunnan Province, P. R. China in March 2022, and was identified by Dr. Honglian Ai. The whole plant specimens were kept at School of Pharmaceutical Sciences, South-Central MinZu University.

Extraction and isolation The whole plants (14.5 kg) after crushing were soaking in 90% MeOH (20 L×5) for a week. The solvent was subsequently removed by a rotary evaporator. The obtained samples were dissolved in water,adjusted pH to 2–3 with weak acids and extracted (each one three times) with petroleum ether, petroleum ether: ethyl acetate = 1:1 and ethyl acetate respectively. The pH was adjusted to 7–8 after removing the organic layer, and extracted three times with ethyl acetate.This part of the ethyl acetate was collected, and the solvent was removed to obtain the sample, which weighed 32 g. The final ethyl acetate extract was divided into five fractions (A-E) by pass through silica gel (200–300 mesh) column chromatography with the elution gradient of $CHCl_3$-CH_3OH (1:0- 0:1).

Fraction B (9 g) was subjected to MPLC separation using a MeOH–H_2O gradient (5:95 to 100:0, v/v), yielding four subfractions (B-1 to B-4). Subfraction B-1 was further fractionated on Sephadex LH-20 (eluent: MeOH) to afford eight components (B-1–1 to B-1–8). Compound **1** (2.2 mg, t_R = 28 min) was obtained from B-1–6 by purification on a preparative C_{18} HPLC column with an MeCN–H_2O gradient (10:90 to 30:70, v/v). Fraction B-2 was separated on Sephadex LH-20 (MeOH) into four subfractions. Purification of B-2–2 via preparative C_{18} HPLC (MeCN–H_2O, 10:90 to 30:70, v/v) afforded compound **9** (9.9 mg, t_R = 25 min). Fraction B-4 was chromatographed on Sephadex LH-20 (MeOH) to yield four subfractions. B-4–1 was further separated on Sephadex LH-20 (MeOH) into five parts. Purification of B-4–1-4 by preparative C_{18} HPLC (MeCN–H_2O, 10:90 to 30:70, v/v) yielded compound **18** (10 mg, t_R = 28 min). B-4–2 was purified using the same type of column (MeCN–H_2O, 10:90 to 40:60, v/v) to give compounds **4** (2.6 mg, t_R = 41 min) and **11** (3.2 mg, t_R = 44 min). B-4–4 was fractionated by silica gel (200–300 mesh) column chromatography with a $CHCl_3$–MeOH gradient (20:1 to 0:1, v/v), yielding four subfractions. B-4–4-2 was purified by preparative C_{18} HPLC (MeCN–H_2O, 20:80 to 40:60, v/v) to afford compound **3** (2.5 mg, t_R = 34 min).Similarly, B-4–4-4 was processed under analogous conditions (MeCN–H_2O, 10:90 to 35:65, v/v) to yield compound **2** (1.2 mg, t_R = 28 min).

Fraction C (4 g) was fractionated by MPLC using a MeOH–H_2O gradient (5:95 to 100:0, v/v), yielding five subfractions (C-1 to C-5). Subfraction C-2 was further separated on Sephadex LH-20 (eluted with MeOH) into six fractions. C-2–2 was purified by preparative C18 HPLC (MeCN–H_2O, 25:75 to 50:50, v/v) to afford compound **5** (1.0 mg, t_R = 19 min), while C-2–3 was processed under similar conditions (MeCN–H_2O, 30:70 to 50:50, v/v) to yield compound **12** (3.0 mg, t_R = 36 min). C-3 was subjected to MPLC with a MeOH–H_2O gradient (5:95 to 100:0, v/v), yielding five subfractions (C-3–1 to C-3–5). Purification of C-3–2 by preparative C_{18} HPLC (MeCN–H_2O, 10:90 to 30:70, v/v) afforded compounds **14** (1.5 mg, t_R = 18 min), **15** (24 mg, t_R = 44 min), and **16** (5 mg, t_R = 49.5 min). C-4 was chromatographed on Sephadex LH-20 (MeOH) to give seven fractions. From C-4–6, compound **13** (18 mg, t_R = 25 min) was obtained after purification via preparative C_{18} HPLC (MeCN–H_2O, 10:90 to 30:70, v/v). C-5 was fractionated on Sephadex LH-20 (MeOH) into seven subfractions. C-5–6 was

Table 6 Lymphocyte toxicity and proliferative inhibitory activity of isolated compounds

Compounds	CC_{50} (μM)	ConA IC_{50} (μM)	SI	LPS IC_{50} (μM)	SI
1	40.5	15.7	2.6	14.8	2.7
3	57.4	44.1	1.3	3.6	15.8
4	> 100	23.9	> 4	8.4	> 11.8
5	> 100	58.6	> 1	9.1	> 10
6	> 100	> 100	/	22.4	> 4
7	/	/	/	> 100	/
8	/	13.8	/	/	/
9	71.7	> 100	< 1	5.3	13.5
10	96.2	49.8	1.9	14.6	6.6
CSAa	2.9	0.003	> 200	0.123	23.2

[a] Positive control

purified using a preparative C_{18} HPLC column (MeCN–H_2O, 10:90 to 30:70, v/v) to yield compound **17** (10 mg, t_R = 23 min).

Fraction D (11 g) was fractionated by MPLC using a MeOH–H_2O gradient (5:95 to 100:0, v/v) to afford five subfractions (D-1 to D-5). Subfraction D-3 was chromatographed on Sephadex LH-20 (eluent: MeOH), yielding seven fractions. Purification of D-3–2 by preparative C18 HPLC (MeCN–H_2O, 15:85 to 50:50, v/v) afforded compound **6** (2.1 mg, t_R = 21 min). Similarly, D-3–6 was processed under a gradient of MeCN–H_2O (10:90 to 30:70, v/v) to give compound **10** (9.2 mg, t_R = 38 min). D-4 was separated on Sephadex LH-20 (MeOH) into four fractions. From D-4–2, compound **22** (5.1 mg, t_R = 27 min) was obtained after purification via preparative C18 HPLC (MeCN–H_2O, 10:90 to 30:70, v/v). D-5 was fractionated on Sephadex LH-20 (MeOH) to give ten subfractions. D-5–3 was purified using a preparative C18 HPLC column (MeCN–H_2O, 10:90 to 30:70, v/v) to yield compounds **7** (1.0 mg, t_R = 51 min) and **8** (3.8 mg, t_R = 56 min). D-5–5 was subjected to the same type of column (MeCN–H_2O, 10:90 to 20:80, v/v) to afford compounds **20** (75 mg, t_R = 29 min) and **21** (1.2 mg, t_R = 24 min). Additionally, D-5–8 was purified under conditions of MeCN–H_2O (10:90 to 30:70, v/v) to give compounds **23** (43 mg, t_R = 30 min) and **19** (75 mg, t_R = 34 min).

Ophiorbrevine A **(1):** yellow powder; $[\alpha]_D^{19}$-2.0 (*c* 0.50, MeOH);); UV (MeOH) λ_{max} (log ε) 235 (4.43), 260 (4.41), 325 (4.17) nm; the ^{1}H (600 MHz) and ^{13}C NMR (150 MHz) data (DMSO), see Table 1; HRMS(ESI) *m/z*: $[M+H]^+$ calcd. for $C_{22}H_{19}O_5N_2$ 391.12885; Found 391.19910.

Ophiorbrevine B **(2):** orange powder, $[\alpha]_D^{19}$ + 165.0 (*c* 0.50, MeOH); UV (MeOH) λ_{max} (log ε) 210 (3.86), 240 (3.89), 270 (3.96) nm; the ^{1}H (600 MHz) and ^{13}C NMR (150 MHz) data (DMSO), see Table 1; HRMS(ESI) *m/z*: $[M+H]^+$ calcd. for $C_{22}H_{20}O_4N_2$ 390.14483; Found 390.14465.

Ophiorbrevine C **(3):** yellow powder, $[\alpha]_D^{23}$ –268.0 (*c* 0.50, MeOH); UV (MeOH) λ_{max} (log ε) 225 (4.38), 270 (3.87) nm; the ^{1}H (600 MHz) and ^{13}C NMR (150 MHz) data ($CDCl_3$), see Table 1; HRMS(ESI) *m/z*: $[M+H]^+$ calcd. for $C_{19}H_{20}N_3$ 290.16517; Found 290.16501.

Ophiorbrevine D **(4):** yellow powder, $[\alpha]_D^{22}$ –8.0 (*c* 0.50, MeOH); UV (MeOH) λ_{max} (log ε) 235 (4.44), 285 (4.04), 340 (3.65) nm; the ^{1}H (600 MHz) and ^{13}C NMR (150 MHz) data (CD_3OD), see Table 2; HRMS(ESI) *m/z*: $[M+H]^+$ calcd. for $C_{19}H_{23}N_2O_2$ 311.17540; Found 311.17517.

Ophiorbrevine E **(5):** yellow powder, $[\alpha]_D^{23}$ + 210.0 (*c* 0.50, MeOH); UV (MeOH) λ_{max} (log ε) 235 (4.33), 295 (4.10) nm; the ^{1}H (600 MHz) and ^{13}C NMR (150 MHz) data (CD_3OD), see Table 2; HRMS(ESI) *m/z*: $[M+H]^+$ calcd. for $C_{19}H_{23}N_2O_3$ 327.17032; Found 327.17010.

Ophiorbrevine F **(6):** yellow powder, $[\alpha]_D^{23}$ –42.0 (*c* 0.50, MeOH); UV (MeOH) λ_{max} (log ε) 220 (4.37), 275 (3.79) nm; the ^{1}H (600 MHz) and ^{13}C NMR (150 MHz) data (CD_3OD), see Table 3; HRMS(ESI) *m/z*: $[M+H]^+$ calcd. for $C_{20}H_{27}O_3N_2$ 343.20162; Found 343.20145.

Ophiorbrevine G **(7):** yellow powder, $[\alpha]_D^{23}$ + 42.0 (*c* 0.50, MeOH); UV (MeOH) λ_{max} (log ε) 225 (3.72), 270 (3.15) nm; the ^{1}H (600 MHz) and ^{13}C NMR (150 MHz) data (CD_3OD), see Table 3; HRMS(ESI) *m/z*: $[M+H]^+$ calcd. for $C_{25}H_{37}O_7N_2$ 477.25953; Found 477.25934.

Ophiorbrevine H **(8):** yellow powder, $[\alpha]_D^{22}$ –20.0 (*c* 0.50, MeOH); UV (MeOH) λ_{max} (log ε) 225 (4.39), 285 (3.90) nm; the ^{1}H (600 MHz) and ^{13}C NMR (150 MHz) data (CD_3OD), see Table 3; HRMS(ESI) *m/z*: $[M+H]^+$ calcd. for $C_{25}H_{37}O_7N_2$ 477.25953; Found 477.26126.

Ophiorbrevine I **(9):** yellow powder, $[\alpha]_D^{22}$ –106.0 (*c* 0.50, MeOH); UV (MeOH) λ_{max} (log ε) 240 (4.25), 270 (4.22), 310 (4.03) nm; the ^{1}H (600 MHz) and ^{13}C NMR (150 MHz) data (CD_3OD), see Table 4; HRMS(ESI) *m/z*: $[M+H]^+$ calcd. for $C_{38}H_{39}O_{14}N_2$ 747.23958; Found 747.24042.

Ophiorbrevine J **(10):** yellow powder, $[\alpha]_D^{23}$ –54.0 (*c* 0.50, MeOH); UV (MeOH) λ_{max} (log ε) 215 (4.59) nm; the ^{1}H (600 MHz) and ^{13}C NMR (150 MHz) data (CD_3OD), see Table 5; HRMS(ESI) *m/z*: $[M+H]^+$ calcd. for $C_{39}H_{43}N_4O_6$ 663.31885; Found 663.31771.

Quantum Chemical Calculations Conformational analyses and ECD calculations were performed using Gaussian 16, Spartan'14, and Chem3D. After determining the relative configuration of the compound according to NMR and MS, the absolute configuration was determined by quantum computing method. Firstly, Spartan'14 was used to search for the dominant conformations of compounds, and the conformational optimization and frequency of multiple low-energy dominant conformations were calculated at the B3LYP/def2svp theoretical level in Gaussian 16. The conformation with a relative energy of less than 3 kcal/mol calculated by the Boltzmann distribution formula was used to calculate the CD using the IEF-PCM solvent model (MeOH) at the theoretical level of wB97XD/Def2sVP. ECD curves of calculated and experimental values were generated by fitting them to SpecDis-1701 software.

Immunosuppressive activity Assays In this experiment, the non-specific toxicity and proliferation response of

mouse lymphocytes were used as a model. The spleens of the mice sacrificed by devertebration were removed and used to prepare a single cell suspension. Red blood cell lysate was used to remove red blood cells and then cell concentration was regulated to obtain different concentrations of mouse spleen lymphocytes required for the experiment.

MTT (Methylthiazolyldiphenyl-tetrazolium bromide) method was used to detect the effect of compounds on the activity of mouse spleen lymphocytes. Mouse spleen lymphocyte suspension (8×10^5/well) was inoculated in 96-well plates, and different concentrations (initial screening concentration: 100, 10, 1 μM, resieve concentration: 100, 50, 25, 12.5, 6.25, 3.125, 1.5625 μM) of compounds were added to a total volume of 200 μL. Positive control drug was immunosuppressant cyclosporin A (CsA, 20, 10, 5, 2.5, 1.25, 0.625, 0.313, 0.156, 0.078, 0.039 μM), cell control was the corresponding solvent, and blank control was culture medium. MTT solution (5 mg/ml) was added 4 h before the end of the culture (37 ℃, 5% CO_2, 48 h). Purple crystals Formazan dissolved in DMSO were added to the plate (150 μL/well) at the end of the culture after removing the supernatant and the OD value was determined under a microplate reader (570 nM).

The effect of compounds on the proliferation of T and B lymphocytes in the spleen of mice was detected by ^{3}H-TdR incorporation method. Mouse spleen lymphocyte suspension (5×10^5/well) was inoculated in 96-well plates, ConA (final concentration 1 μg/ml) or LPS (final concentration 10 μg/ml), and different concentrations (initial screening concentration: 100, 10, 1 μM, resieve concentration: 100, 50, 25, 12.5, 6.25, 3.125, 1.5625 μM) of compounds were added to a total volume of 200 μL. Positive control drug was immunosuppressant cyclosporin A (CsA, 10, 5, 2.5, 1.25, 0.625, 0.313, 0.156, 0.078, 0.039, 0.019 μM), cell control was the corresponding solvent without ConA and LPS, and Stimulation of the drug-free control group. ^{3}H-thymidine nucleotide (25μL/well, 10 μ Ci/ml) was added 8 h before the end of the culture (37 ℃, 5% CO_2, 48 h). Scintillation fluid were added to the cells collected by a cell collector on the fiberglass membrane at the end of the culture and the amount of ^{3}H-TdR incorporated into the DNA of the cell was recorded under a Beta register. The condition of cell proliferation was expressed by cpm values.

Cell viability (%) = (OD_1—OD_3) / (OD_2—OD_3) × 100%, OD_1 was mean of the drug group, OD_2 was mean of the cell control, and OD_3 was the mean of blank control. Inhibition of cell proliferation (%) = (1- (cpm_1—cpm_3) / (cpm_2-cpm_3)) × 100%, cpm_1 was mean of the drug group, cpm_2 was mean of the stimulated control, and cpm_3 was mean of the cell control. Selection index (SI) = CC_{50} (50% Cytotoxic concentration) / IC_{50} (50% inhibitory concentration). SI greater than 10 is considered to have a biological effect. All index check results were processed using Excel 2016 and Graphpad Prism 9.

4 Conclusion

In conclusion, ten new monoterpene indole alkaloids (**1–10**) and 13 known compounds (**11–23**) were isolated from *O. brevidentata*. The structures of all compounds were elucidated through comprehensive spectroscopic analysis, including NMR spectroscopy, high-resolution mass spectrometry, and quantum chemical calculations. Compound **1** features an unprecedented skeleton characterized by a fused 6/5/6/7/6 pentacyclic ring system. Compounds **3–5** and **9** displayed potent inhibitory activity against lipopolysaccharide-induced B cell proliferation, exhibiting IC_{50} values between 3.6 and 9.1 μM along with excellent selectivity (SI > 10), indicating their potential as immunosuppressive agents.

Supplementary Information

The online version contains supplementary material available at https://doi.org/10.1007/s13659-025-00575-y.

Supplementary file 1.

Acknowledgements
This work was financially supported by the National Natural Science Foundation of China (82204239), Hubei Province Department of Education Scientific Research Program Guidance Project (B2024255), and the Fundamental Research Funds for the South-Central MinZu University (YZY24019).

Author contributions
Fan Xu and Zheng-Hui Li have authors contributed equally to this work. The author(s) read and approved the final manuscript.

Funding
National Natural Science Foundation of China, 82204239, baobao shi, Hubei Province Department of Education Scientific Research Program Guidance Project, B2024255, baobao shi, Fundamental Research Funds for the South-Central MinZu University, YZY24019, baobao shi

Data availability
All data generated and analyzed during this study are included in this published article and its Additional file.

Declarations

Conflict of interest
The authors declare that they have no known competing financial interests or personal relationships that could have appeared to influence the work reported in this paper.

Author details
[1]School of Pharmaceutical Sciences, South-Central Minzu University, Wuhan 430074, People's Republic of China. [2]International Cooperation Base for Active Substances in Traditional Chinese Medicine in Hubei Province, School of Pharmaceutical Sciences, South-Central Minzu University, Wuhan 430074, People's Republic of China.

Received: 4 September 2025 Accepted: 27 November 2025
Published online: 11 January 2026

References

1. Wijeyesinghe S, Beura LK, Pierson MJ, Stolley JM, Adam OA, Ruscher R, et al. Expansible residence decentralizes immune homeostasis. Nature. 2021;592(7854):457.
2. Pisetsky DS. Pathogenesis of autoimmune disease. Nat Rev Nephrol. 2023;19(8):509–24.
3. Fugger L, Jensen LT, Rossjohn J. Challenges, progress, and prospects of developing therapies to treat autoimmune diseases. Cell. 2020;181(1):63–80.
4. Song Y, Li J, Wu Y. Evolving understanding of autoimmune mechanisms and new therapeutic strategies of autoimmune disorders. Signal Transduct Target Ther. 2024;9(1):263.
5. Wu Y, Huang YP, Wu Y, Sun JH, Xie QB, Yin G. Systemic immune-inflammation index as a versatile biomarker in autoimmune disorders: insights from rheumatoid arthritis, lupus, and spondyloarthritis. Front Immunol. 2025;16:1621209.
6. Bhat R, Tonutti A, Timilsina S, Selmi C, Gershwin ME. Perspectives on mycophenolate mofetil in the management of autoimmunity. Clin Rev Allergy Immunol. 2023;65(1):86–100.
7. Gabrielli F, Bernasconi E, Toscano A, Avossa A, Cavicchioli A, Andreone P, et al. Side effects of immunosuppressant drugs after liver transplant. Pharmaceuticals. 2025;18(3):342.
8. Dobbels F, Moons P, Abraham I, Larsen CP, Dupont L, De Geest S. Measuring symptom experience of side-effects of immunosuppressive drugs: the modified transplant symptom occurrence and distress scale. Transpl Int. 2008;21(8):764–73.
9. Leroy C, Rigot JM, Leroy M, Decanter C, Le Mapihan K, Parent AS, et al. Immunosuppressive drugs and fertility. Orphanet J Rare Dis. 2015;10:136.
10. Taher M, Shaari SS, Susanti D, Arbain D, Zakaria ZA. Genus *Ophiorrhiza*: a review of its distribution, traditional uses, phytochemistry, biological activities and propagation. Molecules. 2020;25(11):2611.
11. Martins D, Nunez CV. Secondary metabolites from Rubiaceae species. Molecules. 2016;20(7):13422–95.
12. Shi BB, Ai HL, Duan KT, Feng T, Liu JK. Ophiorrhines F and G, key biogenetic intermediates of ophiorrhine alkaloids from *Ophiorrhiza japonica* and their immunosuppressant activities. J Nat Prod. 2022;85(2):453–7.
13. Shi BB, Zhang GR, Li ZH, Liu JK. Three new oxygenated yohimbane-type alkaloids from *Ophiorrhiza japonica*. Fitoterapia. 2023;166:105442.
14. Shi BB, Xu F, Zhang GR, He Y, Liu Q, Feng ML, et al. Glucoconjugated monoterpene indole alkaloids with xanthine oxidase inhibitory activity from *Ophiorrhiza japonica*. Phytochemistry. 2024;224:114169.
15. Feng T, Duan KT, He SJ, Wu B, Zheng YS, Ai HL, et al. Ophiorrhines A and B, two immunosuppressive monoterpenoid indole alkaloids from *Ophiorrhiza japonica*. Org Lett. 2018;20(24):7926–8.
16. Zhang GJ, Hu F, Jiang H, Dai LM, Liao HB, Li N, et al. Mappianines A-E, structurally diverse monoterpenoid indole alkaloids from *Mappianthus iodoides*. Phytochemistry. 2018;145:68–76.
17. Rolfsen WN, Olaniyi AA, Verpoorte R, Bohlin L. Some new decussine type alkaloids from *Strychnos decussata*, *Strychnos dale* and *Strychnos elaeocarpa*. J Nat Prod. 1981;44(4):415–21.
18. Kato L, de Oliveira CMA, Faria EO, Ribeiro LC, Carvalho BG, da Silva CC, et al. Antiprotozoal alkaloids from *Psychotria prunifolia* (Kunth) Steyerm. J Braz Chem Soc. 2012;23(2):355–60.
19. Kutney JP, Brown RT. The structural elucidation of sitsirikine, dihydrositsirikine and isositsirikine. Three new alkaloids from *Vinca rosea Linn*. Tetrahedron. 1966;22(1):321–36.
20. Levesque J, Jacquesy R, Foucher JP. Alcoyl-gluco-alcaloides: nouveaux composes isoles de pauridiantha lyalii brem (rubiacees). Tetrahedron. 1982;38(10):1417–24.
21. Onozawa T, Kitajima M, Kogure N, Peerakam N, Santiarworn D, Takayama H. A cyclopeptide and a tetrahydroisoquinoline alkaloid from *Ophiorrhiza nutans*. J Nat Prod. 2017;80(7):2156–60.
22. Kan-fan C, Zuanazzi JA, Quirion JC, Husson HP, Henriques A. Deppeaninol, a new β-carboline alkaloid from *Deppea blumenaviensis* (Rubiaceae). Nat Prod Res. 1995;7(4):317–21.
23. Lin SZ, Deiana L, Tseggai A, Córdova A. Concise total synthesis of dihydrocorynanthenol, protoemetinol, protoemetine, 3-epi-Protoemetinol and emetine. Eur J Org Chem. 2012;2012(2):398–408.
24. Brandt V, Tits M, Geerlings A, Frédérich M, Penelle J, Delaude C, et al. β-Carboline glucoalkaloids from *Strychnos mellodora*. Phytochemistry. 1999;51(8):1171–6.
25. Lamidi M, Ollivier E, Mahiou V, Faure R, Debrauwer L, Nze Ekekang L, et al. Gluco-indole alkaloids from the bark of *Nauclea diderrichii*. ^{1}H and ^{13}C NMR assignments of 3α-5α-tetrahydrodeoxycordifoline lactam and cadambine acid. Magn Reson Chem. 2005;43(5):427–9.
26. Morita H, Ichihara Y, Takeya K, Watanabe K, Itokawa H, Motidome M. A new indole alkaloid glycoside from the leaves of *Palicourea marcgravii*. Planta Med. 1989;55(3):288–9.
27. Zhang Z, ElSohly HN, Jacob MR, Pasco DS, Walker LA, Clark AM. New indole alkaloids from the bark of *Nauclea orientalis*. J Nat Prod. 2001;64(8):1001–5.
28. Itoh A, Tanahashi T, Nagakura N, Nishi T. Two chromone-secoiridoid glycosides and three indole alkaloid glycosides from *Neonauclea sessilifolia*. Phytochemistry. 2003;62(3):359–69.
29. Berger A, Kostyan MK, Klose SI, Gastegger M, Lorbeer E, Brecker L, et al. Loganin and secologanin derived tryptamine-iridoid alkaloids from *Palicourea crocea* and *Palicourea padifolia* (Rubiaceae). Phytochemistry. 2015;116:162–9.
30. Xiao XB, Lin YX, Xu GB, Gong XB, Gu Y, Tong JF, et al. Two new cytotoxic alkaloids from *Mappianthus iodoides* Hand Mazz. Helv Chim Acta. 2011;94(9):1594–9.
31. Arbain D, Putra DP, Sargent MV. The alkaloids of *Ophiorrhiza filistipula*. Aust J Chem. 1993;46(7):977–85.
32. Muangrom W, Bacher M, Berger A, Valant-Vetschera K, Vajrodaya S, Schinnerl J. A novel tryptophan-derived alkaloid and other constituents from *Guettarda speciosa* (Rubiaceae: Cinchonoideae–Guettardeae). Biochem Syst Ecol. 2021;95:104239.
33. Wang B, Dai Z, Liu L, Wei X, Zhu PF, Yu HF, et al. Indole glycosides from aqueous fraction of *Strychnos nitida*. Nat Prod Bioprospect. 2016;6(6):285–90.
34. Cardoso CL, Siqueira Silva DH, Tomazela DM, Verli H, Young MC, Furlan M, et al. Turbinatine, a potential key intermediate in the biosynthesis of corynanthean-type indole alkaloids. J Nat Prod. 2003;66(7):1017–21.

Publisher's Note